 doi:10.20944/preprints202001.0130.v1

Article

Inter-Molecular Electrostatic Interactions Stabilizing the Structure of the PD-1/PD-L1 Axis: A Structural Evolutionary Perspective

Wei Li [1]*

[1] Institute of Special Environment Medicine, Nantong University, No. 9, Seyuan Road, Nantong City, Jiangsu Province, P. R. China; wli148@aucklanduni.ac.nz

* Correspondence: wli148@aucklanduni.ac.nz

Abstract: PD-1/PD-L1 axis is one key therapeutic target against tumor cell immune escape. Structurally essential to the PD-1/PD-L1-linked immune escape is the binding interface of the PD-1/PD-L1 complex structure. Incorporating currently available PD-1/PD-L1-related experimental structures, this article unveils two sets of experimentally observed inter-molecular electrostatic interactions which stabilize the binding interface of the PD-1/PD-L1 complex structure. For the first time, this article proposes an evolutionary structural hypothesis that, as a result of natural selection, PD-1 is able to genetically mutate itself to structurally disrupt the PD-1/PD-L1 axis towards the restoration of T cell-mediated anti-tumor immunity.

Keywords: PD-1; PD-L1; Cancer-linked genetic mutation; Electrostatic repulsion; Structural evolution

1. Introduction

The PD-1/PD-L1 axis is a pivotal component of tumor cell immune escape mechanism, where the engagement of PD-L1 (on tumor cells) to PD-1 (on T cells) exhausts T cell-mediated anti-tumor immunity [1,2]. To counteract PD-1/PD-L1-linked tumor cell immune escape, one option is the dissociation of the two cell membrane-bound immune checkpoints, i.e., the disruption of the structural bond along the PD-1/PD-L1 axis, which is to be broken at the interface of tumor and T cells, such that the immune system restores its capacity to recognize and kill tumor cells [3–5]. For example, to restore T cell-mediated anti-tumor immunity, targeting the PD-1/PD-L1 axis using checkpoint inhibitors (antibodies against PD-1 or PD-L1, or soluble PD-1 molecules with high affinity to PD-L1) allows tumor cells to be detected and attacked by T cells, which has emerged as a potentially feasible strategy for the treatment of tumors [6–10]. Nevertheless, clinical responses are mixed, highlighting the need for further investigation into the structural aspects of the PD-1-PD-L1 axis in tumor cell immune escape [11–14].

Therefore, this article incorporates currently available PD-1/PD-L1-related experimental structures (as of December 24, 2019) [15] and experimentally observed cancer-linked genetic mutation of the two immune checkpoints, and puts forward a set of in silico electrostatic analysis of all PD-1-PD-L1 complex structures (as of December 24, 2019), aiming at deciphering and visualizing the inter-molecular electrostatic interactions that are instrumental in the structural stability of the PD-1/PD-L1 complex.

Preprints (www.preprints.org) | NOT PEER-REVIEWED | Posted: 12 January 2020 doi:10.20944/preprints202001.0130.v1

2. Materials and Methods

2.1. Experimentally determined PD-1-PD-L1 structures

As of December 24, 2019, a total of 52 PD-1- and/or PD-L1-related structures (Supplementary file **supp.pdf**) have been experimentally determined and deposited in PDB [15].

PDB ID	Chain ID	Protein Name (Synonym)
3BIK	A	PD-L1 (CD274)
3BIK	B	PD-1 (CD279)
3BIK	C	PD-1 (CD279)
3SBW	A	PD-1 (CD279)
3SBW	B	PD-1 (CD279)
3SBW	C	PD-L1 (CD274)
4ZQK	A	PD-L1 (CD274)
4ZQK	B	PD-1 (CD279)
5IUS	A	PD-1 (CD279)
5IUS	B	PD-1 (CD279)
5IUS	C	PD-L1 (CD274)
5IUS	D	PD-L1 (CD274)

Table 1. Experimental structures of the PD-1-PD-L1 complex in PDB as of December 24, 2019, along with their respective PDB IDs, chain IDs and (alternative) protein names.

Among the 52 PD-1- and/or PD-L1-related structures, four represent the PD-1-PD-L1 complex structure (Table 1), which are to be analysed in detail and discussed further below.

2.2. Structural analysis of the PD-1-PD-L1 complex

First, the InterProSurf server (http://curie.utmb.edu/pdbcomplex.html) [16] was used to identify interfacial amino acid residues of the PD-1-PD-L1 complex structures (Table 1). Subsequent structural analysis, including salt bridging and hydrogen bonding analysis [17], was performed as described previously for all 52 experimentally determined PD-1-PD-L1 complex structures as of December 24, 2019.

3. Results

To investigate the structural stability of the binding interface of the PD-1/PD-L1 complex structure, it is necessary to first chart out the entire interfacial salt bridging and hydrogen bonding networks of the two immune checkpoints. Thus, an set of residue-specific structural analysis was carried out at the binding interface of the PD-1-PD-L1 complex structure. Specifically, an amino acid residue is taken into further consideration of subsequent structural analysis only when it fulfills no less than three of the four criteria below,

1. it is associated with at least one cancer-linked mutation (BioMuta).
2. it is located at the interface of the PD-1-PD-L1 complex (InterProSurf).
3. it is involved in the salt bridging network [17] at the PD-1-PD-L1 binding interface.
4. it is involved in the hydrogen bonding network [17] at the PD-1-PD-L1 binding interface.

3.1. The cervical cancer-linked Glu136Gln mutation of PD-1

According to the InterProSurf interfacial residue analysis [16], Glu136 of PD-1 sits at the interface of the four PD-1-PD-L1 complex structures (Table 1). Further structural analysis reveals that Glu136 and Ser137 of PD-1 forms an intra-molecular hydrogen bond within PD-1 (PDB ID: 2M2D, Table 2). Moreover, Glu136 and Arg139 of PD-1 forms a stable intra-molecular salt bridge within PD-1 (PDB IDs: 2M2D and 5GGR, supplementary file **Glu136.pdf**).

Preprints (www.preprints.org) | NOT PEER-REVIEWED | Posted: 12 January 2020 doi:10.20944/preprints202001.0130.v1

PDB	Acceptor (A)	Donor (D)	Hydrogen (H)	D-A (Å)	H-A (Å)	$\angle ADH(°)$
2M2D_25	O, A_GLU_136	OG, A_SER_137	HG, A_SER_137	2.75	1.79	9.71

Table 2. The hydrogen bond formed between Glu136 and Ser 137 of PD-1. In this table, 2M2D_25 represents the 25th structural model in the NMR ensemble (PDB ID: 2M2D), the residue naming scheme is **Chain ID_residue name_residue number**, $\angle ADH$ represents the angle formed by acceptor (A), donor (D) and hydrogen (H) ($\angle ADH$).

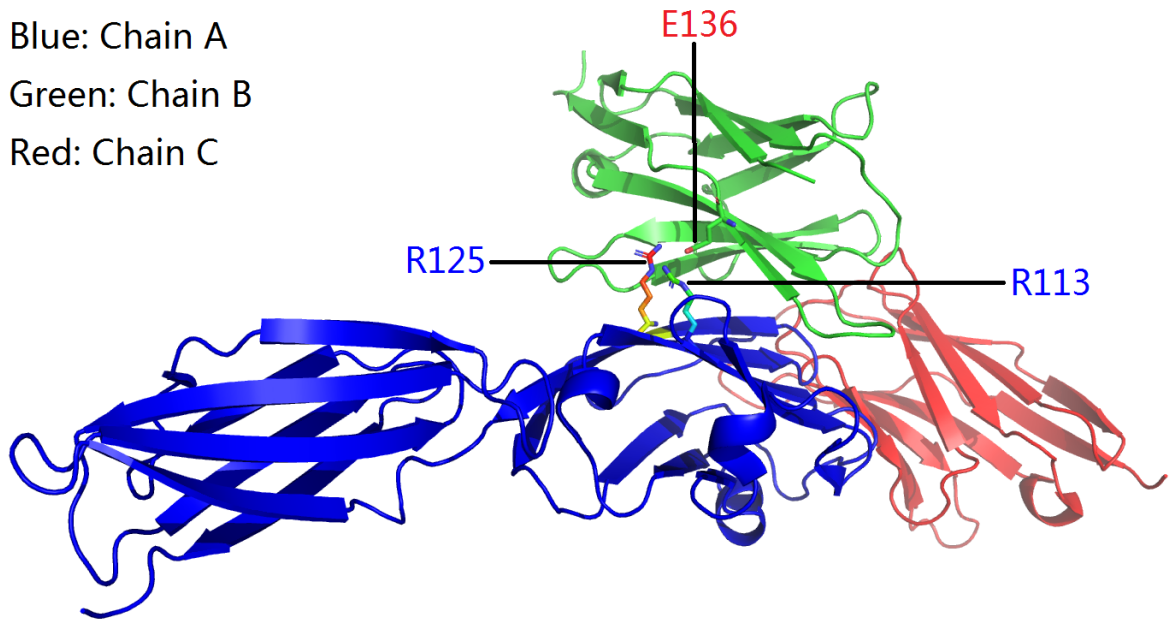

Figure 1. An overview of the structurally identified side chain salt bridges between an amino acid trio, i.e., Glu136 of PD-1 and Arg113 and Arg125 of PD-L1 for PDB ID 3BIK (Table 1).

Interestingly, for the two PD-1-PD-L1 complex structures (3BIK and 4ZQK, Table 1), Glu136 of PD-1 forms salt bridges (Figures 1 and 2) with Arg113 and Arg125 of PD-L1, which both sit at the structural interface of the two immune checkpoints (PDB IDs: 3BIK, 4ZQK and 5IUS, and 3SBW, Table 1), although no cancer-linked mutation was clinically identified yet for Arg113 and Arg125 of PD-L1 as of December 24, 2019.

SB1	Color = Green, Distance = 3.149 Å
Atomic coordinate	ATOM 777 NH2 ARG A 113 12.637 -2.086 -32.968 1.00 70.85 N
Atomic coordinate	ATOM 2538 OE2 GLU B 136 11.442 -1.132 -30.215 1.00 72.18 O
SB2	Color = Blue, Distance= 3.033 Å
Atomic coordinate	ATOM 870 NH2 ARG A 125 14.394 -1.252 -29.687 1.00 69.69 N
Atomic coordinate	ATOM 2537 OE1 GLU B 136 11.832 -1.667 -28.118 1.00 63.00 O
SB3	Color = Red, Distance = 3.001 Å
Atomic coordinate	ATOM 870 NH2 ARG A 125 14.394 -1.252 -29.687 1.00 69.69 N
Atomic coordinate	ATOM 2538 OE2 GLU B 136 11.442 -1.132 -30.215 1.00 72.18 O

Table 3. The structurally identified inter-molecular side chain salt bridges between Glu136 of PD-1 and Arg113 and Arg125 of PD-L1 for PDB ID 3BIK (Table 1). In this table, Color = Green, Color = Blue and Color = Red represent the three interfacial salt bridges as shown in Figure 2 with the corresponding colors, respectively.

Given that Glu136 of PD-1 is associated with the cervical cancer-linked Glu136Gln (E136Q) mutation, this E136Q substitution removes the negatively charged glutamate side chain of Glu136,

Preprints (www.preprints.org) | NOT PEER-REVIEWED | Posted: 12 January 2020 doi:10.20944/preprints202001.0130.v1

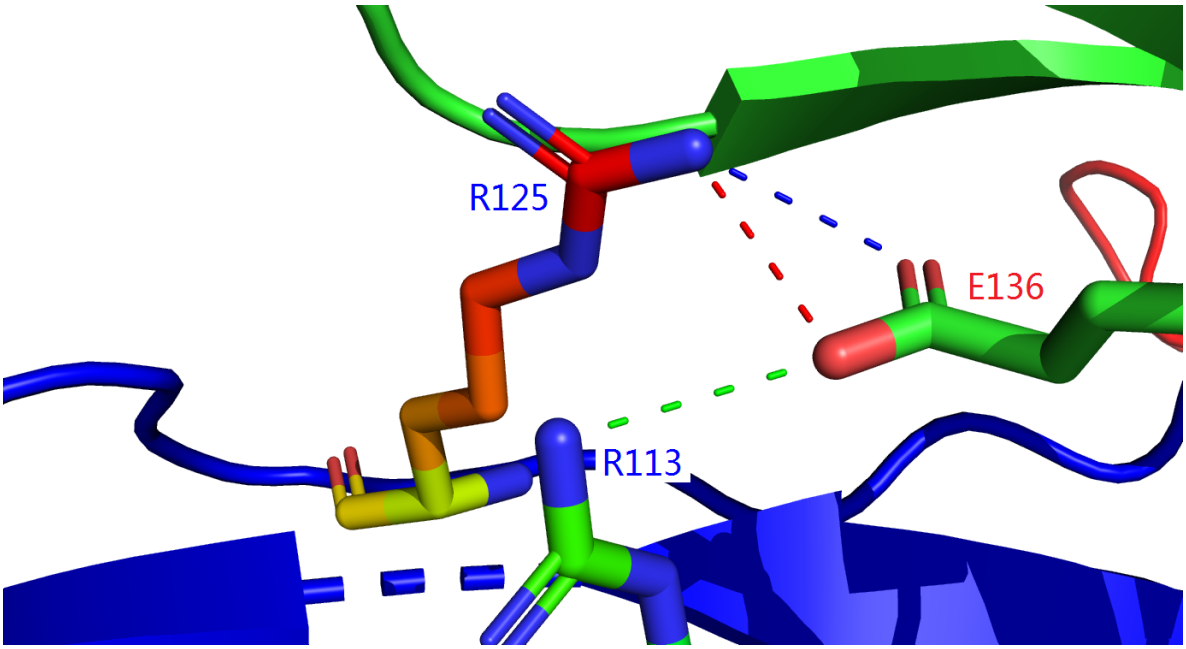

Figure 2. The structurally identified inter-molecular side chain salt bridges between Glu136 of PD-1 and Arg113 and Arg125 of PD-L1 for PDB ID 3BIK). In this figure, the side chain salt bridges are shown as dotted short cylinders with different colors, the details of the salt bridges are included in Table 3.

and installs the neutral side chain group of Gln136, along with the hydrogen with partial positive charge in the side chain NH_2 group of Gln136. Similar to the spinal muscular atrophy-linked binding interface-disrupting Gln136Glu (Q136E) mutation [17], the E136Q substitution here gives rise to a reversal in the charge carried by the side chain of Glu136, shifting the local electrostatic attraction (the side chain salt bridges and hydrogen bond of Gln136 of PD-1, Figures 1 and 2) to local electrostatic repulsion [18,19] between Gln136's side chain (with partial positive charge) and the positively charged side chains of Arg113 and Arg125.

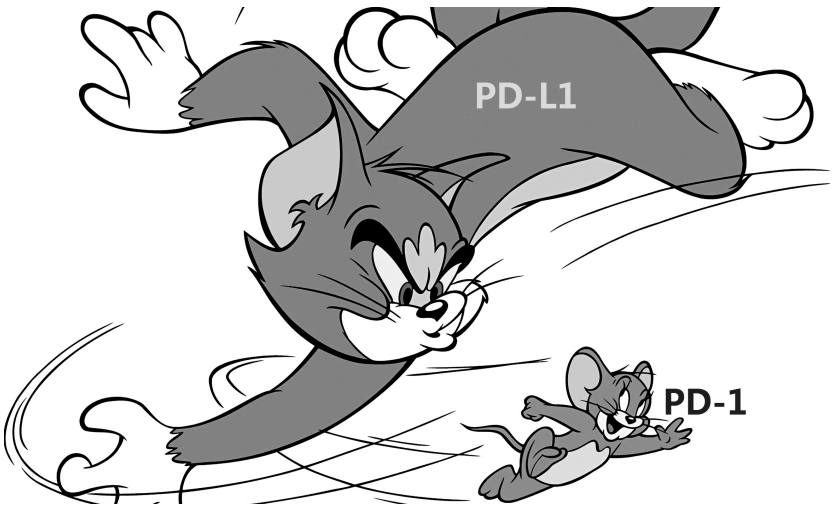

Figure 3. To facilitate tumor cell immune escape, PD-L1 binds to PD-1 as a cat catches hold of a mouse, towards the exhaustion of T cell-mediated anti-tumor immunity [1,2,4,5]. Reproduced with permission from Everett Collection (https://www.everettcollection.com).

Overall, the net structural and functional consequence of this E136Q substitution is the local electrostatic equilibrium perturbation [17] at the binding interface of the PD-1-PD-L1 complex, and as shown in Figure 1, it is likely that this cervical cancer-linked E136Q substitution disrupts the

 doi:10.20944/preprints202001.0130.v1

binding interface of PD-1 and PD-L1, thereby allowing PD-1 to distance itself away from PD-L1, which suppresses the PD-1/PD-L1 axis towards the restoration of T cell-mediated anti-tumor immunity. This structural evolution hypothesis is likened to a situation where PD-L1 (the cat, Figure 3) uses its claws (Arg125 of PD-L1) to catch hold of PD-1 (the mouse, Figure 3) via the Glu136 residue of PD-1 (Figure 2) to facilitate tumor cell immune escape, highlighting the functional importance of the interacting interfacial residues of the PD-1-PD-L1 complex structure [20] On the other hand, however, PD-1 is able to hide itself (via a Glu136Gln substitution) and escape from the recognition (the claw) and binding of PD-L1 (the cat, Figure 3), towards the restoration of T cell-mediated anti-tumor immunity [1,2,4,5].

3.2. The breast cancer-linked Met70Lys mutation of PD-1

As discussed above, Arg125 of PD-L1 is like one claw of the cat (PD-L1, Figure 3), allowing PD-L1 to bind to Glu136 of PD-1 (the mouse, Figures 3, 1 and 2) towards the establishment of the PD-1-PD-L1 axis. After a set of comprehensive structural analysis for Arg125 of PD-L1 (supplementary file **Arg125.pdf**), it turned out that Arg125 allowed PD-L1 to bind to Glu70 of a PD-1 mutant (PDB ID: 5IUS, Table 1), too.

Here, PDB ID 5IUS corresponds to an crystal structure of human PD-L1 in complex with high affinity PD-1 mutant (supplementary file **supp.pdf**). Quite intriguingly, the 70th residue of wild-type PD-1 is methionine (Met, M), which is associated with the breast cancer-linked M70K mutation of PD-1. Therefore, the M70E substitution (PDB ID: 5IUS, Table 1) contributes to the local structural stability and thus high affinity of the PD-1 mutant to PD-L1 as a total of five inter-molecular interfacial salt bridges formed between Glu70 (of PD-1) and Arg125 (of PD-L1) at the binding interface of the two immune checkpoints, as listed in the supplementary file **Arg125.pdf**.

In contrast, however, the breast cancer-linked M70K mutation of PD-1 does exactly the opposite to the structural and functional consequence of the human-introduced M70E mutation, in the sense that the M70K mutation establishes a local electric charge reversal for the side chain of the 70th residue of PD-1 and disrupts the inter-molecular salt bridges at the binding interface of the two immune checkpoints, where the net structural and functional consequence is the local electrostatic energy equilibrium perturbation (if not disruption) [17] at the binding interface of the PD-1-PD-L1 complex.

Overall, the human-introduced M70E and the breast cancer-linked M70K substitutions are like the two sides of one coin, and serve as two excellent examples of how human intervention does exactly the opposite to the effect of genetic mutation-driven natural selection in the structural evolution of PD-1, where its M70K substitution removes the hydrophobic side chain of its Met70 and installs instead a positively charged side chain of at its 70th residue site (Lys70), and thereby establishes a structurally destabilizing electrostatic repulsive force [17–19] between Lys70 (of PD-1) and Arg125 (of PD-L1) at their binding interface. On the other side of the coin, while the M70E substitution of PD-1 removes the hydrophobic side chain of its Met70 and installs instead a negatively charged side chain at its 70th residue site (Glu70), and thereby establishes a structurally stabilizing electrostatic attractive force, i.e., five inter-molecular interfacial salt bridges between Glu70 (of PD-1) and Arg125 (of PD-L1) to further consolidate the PD-1-PD-L1 axis and consequently the tumor cell immune escape mechanism, too.

4. Conclusion

1. This article highlights an amino acid residue trio (Glu136 of PD1 and Arg125 and Arg113 of PD-L1, Figures 1), which are inextricably linked to inter-molecular electrostatic interactions towards the structural stabilization of the PD-1-PD-L1 axis in tumor cell immune escape.
2. This article highlights two cancer-linked genetic mutations of PD-1, i.e., the cervical cancer-linked Glu136Gln(E136Q) mutation of PD-1 and the breast cancer-linked Met70Lys (M70K) mutation of PD-1, which are at play in the inter-molecular electrostatic interactions towards the structural stabilization/destabilization of the PD-1-PD-L1 axis.

Preprints (www.preprints.org) | NOT PEER-REVIEWED | Posted: 12 January 2020 doi:10.20944/preprints202001.0130.v1

3. With the two experimentally observed cancer-linked genetic mutations (E136Q and M70K) of PD-1, this article puts forward an evolutionary structural hypothesis that, from a structural point of view, PD-1 is able to genetically mutate itself (Figures 3) to structurally disrupt the PD-1/PD-L1 axis towards the restoration of T cell-mediated anti-tumor immunity. Specifically, genetic variation-induced electrostatic repulsion [17,18] is involved in the evolutionary suppression of the tumor cell immune escape mechanism, where the electric charge reversal constitutes a functional significant unfavourable electrostatic energy contribution towards the structural perturbation (if not disruption) of the PD-1-PD-L1 complex structure [1,3,4].
4. With this evolutionary structural hypothesis, this article presents further discuss Tyr68 of PD-1 and Asp122 of PD-L1 at the structural interface of the two immune checkpoints, which is to be described in detail below.

5. Discussion

5.1. Tyr68 of PD-1 and Asp122 of PD-L1: a structural evolutionary perspective

As of December 24, 2019, no cancer-linked mutation was clinically identified yet either for Tyr68 of PD-1 or for Asp122 of PD-L1. Nonetheless, both Tyr68 of PD-1 and Asp122 of PD-L1 sit at the binding interface of PD-1 and PD-L1, according to the three experimental structures of PD-1-PD-L1 complex (PDB IDs: 3BIK, 4ZQK and 5IUS, Table 1). In PDB ID 5IUS (Table 1), a Tyr68His (Y68H) substitution was introduced to PD-1 to replace the hydrophobic side chain (of Tyr68) with one positively charged side chain of His68. After the Y68H substitution, three inter-molecular side chain salt bridges (Figures 4 and 5) were formed between His68 of the mutant PD-1 and Asp122 of PD-L1.

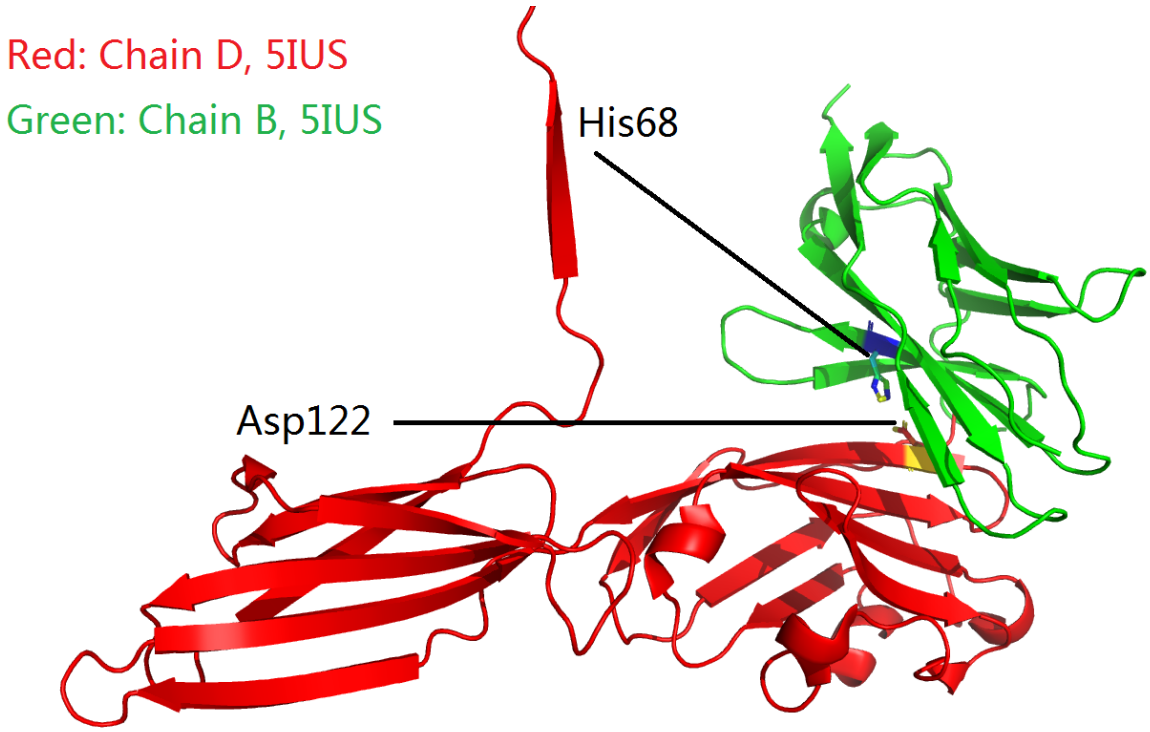

Figure 4. An overview of two salt-bridged amino acid residues at the binding interface of PD-1 (green) and PD-L1 (red) according to their complex structure (PDB ID: 5IUS, Table 1).

From Figure 4, it can be seen that His68 (of mutant PD-1) and Asp122 (of PD-L1) constitute two structurally stabilizing electrostatic clips [17] at the binding interface of the two immune checkpoints. Thus, the Y68H substitution contributes to the local structural stability and consequently high affinity of the PD-1 mutant to PD-L1 as a total of three inter-molecular salt bridges (supplementary file

Preprints (www.preprints.org) | NOT PEER-REVIEWED | Posted: 12 January 2020 doi:10.20944/preprints202001.0130.v1

Asp122.pdf) were formed between the side chains (Figures 4 and 5) of His70 (of PD-1) and Asp122 (of PD-L1).

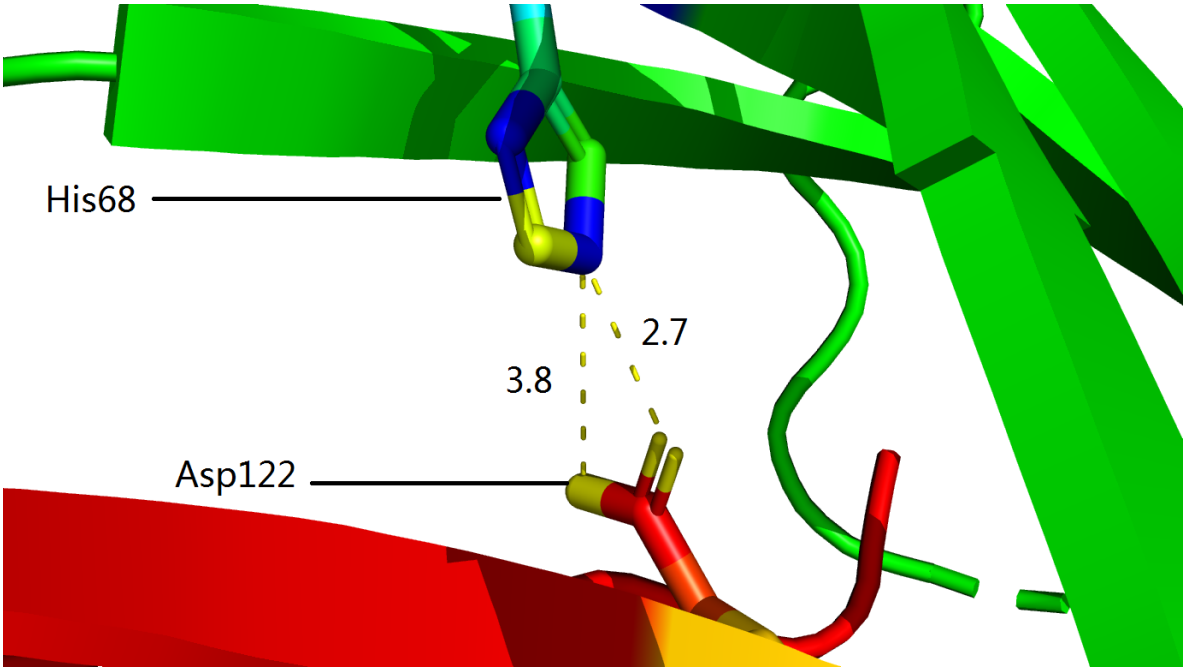

Figure 5. The structurally identified inter-molecular side chain salt bridges between His68 of PD-1 (mutant) and Asp122 of PD-L1 for PDB ID 5IUS). In this figure, the side chain salt bridges are shown as dotted yellow short cylinders, 3.8 represents the distance (3.8 Å) of the salt bridge formed between $N_{\varepsilon 2}$ (blue) of His68 of PD-1 (mutant) and $O_{\delta 2}$ (yellow) of Asp122 of PD-L1, 2.7 represents the distance (2.7 Å) of the salt bridge formed between $N_{\varepsilon 2}$ (blue) of His68 of PD-1 (mutant) and $O_{\delta 1}$ (yellow) of Asp122 of PD-L1 (supplementary file **Asp122.pdf**).

Thus, it is reasonable to not rule out the possibility that a Tyr68Asp (or Tyr68Glu) substitution will take place in future in the scaffold of PD-1 and is clinically identified and linked to cancer patient(s). This prediction stems from the same structural evolutionary hypothesis, where a Tyr68Asp (or Tyr68Glu) substitution of PD-1 is able to establish an electrostatic repulsive force between Asp122 of PD-L1, in addition to removing the three structurally stabilizing inter-molecular side chain salt bridges (Figures 4 and 5) formed between His68 of the mutant PD-1 and Asp122 of PD-L1. On the contrary, when a Tyr68Asp (or Tyr68Glu) substitution of PD-1 does take place in future, then this structural evolutionary hypothesis predicts again that an Asp122Arg (or Asp122Lys) substitution of PD-L1 will take place, too, towards the restoration of structurally stabilizing inter-molecular electrostatic interactions between the two immune checkpoints. Similarly, this situation is likened to that in Figure 3, where the cat (PD-L1 of tumor cell) uses its claw to catch hold of the mouse, i.e., PD-1 of T cell, towards the exhaustion of T cell-mediated anti-tumor immunity [1,2,4,5].

5.2. Application of gene-editing technologies to structurally disrupt the PD-1-PD-L1 axis

As discussed above, the PD-1-PD-L1 axis is but one of the many tumor immune escape mechanisms, which makes tumor a difficult foe for the immune system, and explains at least partly why PD-1/PD-L1 antibody-based clinical responses are mixed [11–13], highlighting the need to tackle tumors from multiple angles, such that there is less chance for it to acquire resistance and avoid elimination by the immune system. Similarly, if a tumor is targeted and treated precisely, there is less chance for adverse effects to take place. Thus, against the PD-1/PD-L1-linked tumor cell immune escape, this structural evolutionary mechanism provides a novel perspective for the application of gene-editing [8,21–23] technologies in the treatment of tumors, since the engagement of PD-L1 (or even PD-L2, supplementary file **supp.pdf**) (on tumor cells) to PD-1 (on T cells) is central to the PD-1/PD-L1

axis, which causes T cell exhaustion, a hyporesponsive state of T cells in tumor microenvironment, with increased inhibitory receptors, decreased effector cytokines and impaired cytotoxicity [24].

For instance, since Arg125 and Arg133 are like two claws of the cat (Figure 3), site-specific genetic mutations such as Arg125Glu (R125E) and Arg113 (R113E) for PD-L1 are able to establish two structurally destabilizing electrostatic repulsive forces between them and Glu136 of PD-1, because not only are the two claws removed to prevent PD-L1 from binding to PD-1 (Figure 3), but also is the cat (PD-L1) energetically reluctant to catch hold of the mouse (PD-1, Figure 3) due to the electrostatic repulsions between its Glu136 and Glu113 and Glu125 of PD-L1, and also are the approaching PD-1 molecules trying to stay further away from PD-L1 due to the electrostatic repulsions between Glu136 of PD-1 and Glu113 and Glu125 of PD-L1, too.

Author Contributions: Cconceptualization, W.L.; methodology, W.L.; software, W.L.; validation, W.L.; formal analysis, W.L.; investigation, W.L.; resources, W.L.; data curation, W.L.; writing–original draft preparation, W.L.; writing–review and editing, W.L.; visualization, W.L.; supervision, W.L.; project administration, W.L.; funding acquisition, not applicable.

Funding: This research received no external funding.

Acknowledgments: I thank Dr. Yongdong Niu (Department of Pharmacology, Shantou University Medical College) for his insights on this topic.

Conflicts of Interest: The author declares no conflict of interest.

1. Beatty, G.L.; Gladney, W.L. Immune Escape Mechanisms as a Guide for Cancer Immunotherapy. *Clinical Cancer Research* **2014**, *21*, 687–692. doi:10.1158/1078-0432.ccr-14-1860.
2. Salmaninejad, A.; Valilou, S.F.; Shabgah, A.G.; Aslani, S.; Alimardani, M.; Pasdar, A.; Sahebkar, A. PD-1/PD-L1 pathway: Basic biology and role in cancer immunotherapy. *Journal of Cellular Physiology* **2019**, *234*, 16824–16837. doi:10.1002/jcp.28358.
3. Chen, L.; Han, X. Anti–PD-1/PD-L1 therapy of human cancer: past, present, and future. *Journal of Clinical Investigation* **2015**, *125*, 3384–3391. doi:10.1172/jci80011.
4. Jiang, X.; Wang, J.; Deng, X.; Xiong, F.; Ge, J.; Xiang, B.; Wu, X.; Ma, J.; Zhou, M.; Li, X.; Li, Y.; Li, G.; Xiong, W.; Guo, C.; Zeng, Z. Role of the tumor microenvironment in PD-L1/PD-1-mediated tumor immune escape. *Molecular Cancer* **2019**, *18*. doi:10.1186/s12943-018-0928-4.
5. Constantinidou, A.; Alifieris, C.; Trafalis, D.T. Targeting Programmed Cell Death -1 (PD-1) and Ligand (PD-L1): A new era in cancer active immunotherapy. *Pharmacology & Therapeutics* **2019**, *194*, 84–106. doi:10.1016/j.pharmthera.2018.09.008.
6. Fusi, A.; Festino, L.; Botti, G.; Masucci, G.; Melero, I.; Lorigan, P.; Ascierto, P.A. PD-L1 expression as a potential predictive biomarker. *The Lancet Oncology* **2015**, *16*, 1285–1287. doi:10.1016/s1470-2045(15)00307-1.
7. Cyranoski, D. CRISPR gene-editing tested in a person for the first time. *Nature* **2016**, *539*, 479–479. doi:10.1038/nature.2016.20988.
8. Zhan, T.; Rindtorff, N.; Betge, J.; Ebert, M.P.; Boutros, M. CRISPR/Cas9 for cancer research and therapy. *Seminars in Cancer Biology* **2018**. doi:10.1016/j.semcancer.2018.04.001.
9. Liu, Y.; Wu, L.; Tong, R.; Yang, F.; Yin, L.; Li, M.; You, L.; Xue, J.; Lu, Y. PD-1/PD-L1 Inhibitors in Cervical Cancer. *Frontiers in Pharmacology* **2019**, *10*. doi:10.3389/fphar.2019.00065.
10. Li, Y.; Liang, Z.; Tian, Y.; Cai, W.; Weng, Z.; Chen, L.; Zhang, H.; Bao, Y.; Zheng, H.; Zeng, S.; Bei, C.; Li, Y. High-affinity PD-1 molecules deliver improved interaction with PD-L1 and PD-L2. *Cancer Science* **2018**, *109*, 2435–2445. doi:10.1111/cas.13666.
11. Pauken, K.E.; Wherry, E.J. Overcoming T cell exhaustion in infection and cancer. *Trends in Immunology* **2015**, *36*, 265–276. doi:10.1016/j.it.2015.02.008.
12. Liang, Z.; Tian, Y.; Cai, W.; Weng, Z.; Li, Y.; Zhang, H.; Bao, Y.; Li, Y. High-affinity human PD-L1 variants attenuate the suppression of T cell activation. *Oncotarget* **2017**, *8*. doi:10.18632/oncotarget.21729.
13. Pawelec, G. Is There a Positive Side to T Cell Exhaustion? *Frontiers in Immunology* **2019**, *10*. doi:10.3389/fimmu.2019.00111.

14. Wang, Y.; Zhou, S.; Yang, F.; Qi, X.; Wang, X.; Guan, X.; Shen, C.; Duma, N.; Aguilera, J.V.; Chintakuntlawar, A.; Price, K.A.; Molina, J.R.; Pagliaro, L.C.; Halfdanarson, T.R.; Grothey, A.; Markovic, S.N.; Nowakowski, G.S.; Ansell, S.M.; Wang, M.L. Treatment-Related Adverse Events of PD-1 and PD-L1 Inhibitors in Clinical Trials. *JAMA Oncology* **2019**, *5*, 1008. doi:10.1001/jamaoncol.2019.0393.
15. Berman, H.; Henrick, K.; Nakamura, H. Announcing the worldwide Protein Data Bank. *Nature Structural & Molecular Biology* **2003**, *10*, 980–980. doi:10.1038/nsb1203-980.
16. Negi, S.S.; Schein, C.H.; Oezguen, N.; Power, T.D.; Braun, W. InterProSurf: a web server for predicting interacting sites on protein surfaces. *Bioinformatics* **2007**, *23*, 3397–3399. doi:10.1093/bioinformatics/btm474.
17. Li, W. How do SMA-linked mutations of *SMN1* lead to structural/functional deficiency of the SMA protein? *PLOS ONE* **2017**, *12*, e0178519. doi:10.1371/journal.pone.0178519.
18. Li, W.; Shi, G. How $Ca_V1.2$-bound verapamil blocks Ca^{2+} influx into cardiomyocyte: Atomic level views. *Pharmacological Research* **2019**, *139*, 153–157. doi:10.1016/j.phrs.2018.11.017.
19. Li, W. Characterising the interaction between caenopore-5 and model membranes by NMR spectroscopy and molecular dynamics simulations. PhD thesis, University of Auckland, 2016.
20. Magnez, R.; Thiroux, B.; Taront, S.; Segaoula, Z.; Quesnel, B.; Thuru, X. PD-1/PD-L1 binding studies using microscale thermophoresis. *Scientific Reports* **2017**, *7*. doi:10.1038/s41598-017-17963-1.
21. Tsai, S.Q.; Nguyen, N.T.; Malagon-Lopez, J.; Topkar, V.V.; Aryee, M.J.; Joung, J.K. CIRCLE-seq: a highly sensitive in vitro screen for genome-wide CRISPR–Cas9 nuclease off-targets. *Nature Methods* **2017**, *14*, 607–614. doi:10.1038/nmeth.4278.
22. Zuo, E.; Sun, Y.; Wei, W.; Yuan, T.; Ying, W.; Sun, H.; Yuan, L.; Steinmetz, L.M.; Li, Y.; Yang, H. Cytosine base editor generates substantial off-target single-nucleotide variants in mouse embryos. *Science* **2019**, p. eaav9973. doi:10.1126/science.aav9973.
23. Yang, J.; Hu, L. Immunomodulators targeting the PD-1/PD-L1 protein-protein interaction: From antibodies to small molecules. *Medicinal Research Reviews* **2018**, *39*, 265–301. doi:10.1002/med.21530.
24. Jiang, Y.; Li, Y.; Zhu, B. T-cell exhaustion in the tumor microenvironment. *Cell Death & Disease* **2015**, *6*, e1792–e1792. doi:10.1038/cddis.2015.162.